24th INTERNATIONAL CONGRESS ON SOUND AND VIBRATION
23–27 July 2017, London

VIBRATION BAND GAPS OF ONE-DIMENSIONAL PHONONIC CRYSTALS USING WAVE FINITE ELEMENT METHOD

Hong Wu, Hao xu, Fusheng Sui, Guofeng Bai

Key Laboratory of Noise and Vibration Research, Institute of Acoustics, University of Chinese Academy of Sciences, China
email: bgf@mail.ioa.ac.cn

Phononic crystals are widely researched and applied nowadays. Their dynamical performance need to be investigated for the purpose of design and optimization. In this paper, wave finite element method (WFEM) is employed to acquire the vibration band gaps of one-dimensional phononic crystals. Because of the periodic characteristics of the phononic crystals, only one unit cell needs to meshed, the FE model in which the mass and stiffness matrices are typically extracted using a conventional FE package. Band gaps can be obtained from the eigenvalues of the segment transfer matrix, other properties of the structures are also derived from the formulation. Some numerical results are presented and compared with theory results, a good agreement is observed. This work provides an effective technique to analyse the dynamical characteristics of metamaterial structures.

Keywords: vibration band gap; phononic crystals; WFEM

1. Introduction

The study of phononic materials and structures is an emerging discipline that lies at the crossroads of vibration and acoustics engineering and condensed matter physics. One-dimensional phononic crystals that can be obtained by repeating a single unit cell are widely employed in various engineering domains. The wide application and rich dynamic behaviours of phononic crystals have attracted lots of researches in these years[1].

In recent years, the field of periodic structure has experienced a resurgence with the introduction of phononic crystals, the band gap and cavity mode in phononic crystal strip waveguides was studied by Li [2]. The application of the phononic crystals is also widely, Yanfei Li[3] controlled the low-frequency noise by design the acoustic metamaterials successfully.

In this paper, we study three types of vibration band gaps of one-dimensional phononic crystals. In section 2, finite element displacement method is employed to obtain the mass and stiffness matrices of the structures. The formulation of WFEM on one-dimensional phononic crystals is proposed in section3. Results and discussions of the band structure are presented in section 4. A short summary is given in section 5.

2. Finite element method for modelling 1D structures

In order to calculate the dynamic properties of the phononic crystals, the mass and stiffness matrices of unit cell must be obtained.

This section describes how to obtain the mass and stiffness matrices of one-dimensional single element by finite element displacement method[4].

All vibration modes of one-dimensional element are given in Fig.1. Axial vibration mode is shown in Fig.1a, torsional vibration mode is shown in Fig.1b and bending vibration mode is shown in Fig.1c.

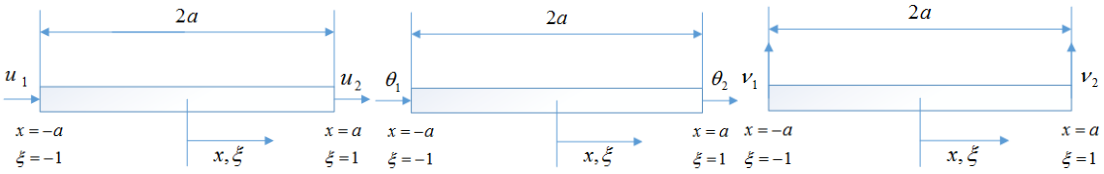

a) Axial b) Torsional c) Bending

Figure 1 Vibration modes of one-dimensional element

2.1 Axial vibration

The deformation of an axial element is:

$$u = N_1(\xi)u_1 + N_2(\xi)u_2 \tag{1}$$

where

$$\mathrm{N}_i(\xi) = \frac{1}{2}(1+\xi_i\xi) \quad (\xi_1 = -1, \xi_2 = 1) \tag{2}$$

The expression Eq. (1) can be rewritten in matrix form as follows:

$$u = \lfloor \mathrm{N}_1(\xi) \quad \mathrm{N}_2(\xi) \rfloor \begin{bmatrix} u_1 \\ u_2 \end{bmatrix} = \lfloor \mathrm{N}(\xi) \rfloor \{u\}_e \tag{3}$$

where the shape function of the axial element is:

$$\lfloor \mathrm{N}(\xi) \rfloor = \lfloor \mathrm{N}_1(\xi) \quad \mathrm{N}_2(\xi) \rfloor \tag{4}$$

The energy expressions for the single element shown in Fig.1a are:

$$\begin{aligned} T_e &= \frac{1}{2}\int_{-a}^{+a} \rho A \dot{u}^2 \\ U_e &= \frac{1}{2}\int_{-a}^{+a} EA\left(\frac{\partial u}{\partial x}\right)^2 dx \end{aligned} \tag{5}$$

Substituting the displacement expression into the kinetic energy and the strain energy gives:

$$T_e = \frac{1}{2}\{\dot{u}\}_e^{\mathrm{T}}[m]_e\{\dot{u}\}_e \tag{6}$$

where

$$[m]_e = \rho A a \int_{-1}^{+1} \lfloor \mathrm{N}(\xi) \rfloor^{\mathrm{T}} \lfloor \mathrm{N}(\xi) \rfloor \mathrm{d}\xi \tag{7}$$

Which is referred to as the ‘element mass matrix’,

$$U_e = \frac{1}{2}\{u\}_e^{\mathrm{T}}[\mathrm{K}]_e\{u\}_e \tag{8}$$

where

$$[\mathrm{K}]_e = \frac{EA}{a}\int_{-1}^{+1} \lfloor \mathrm{N}'(\xi) \rfloor^{\mathrm{T}} \lfloor \mathrm{N}'(\xi) \rfloor \mathrm{d}\xi \tag{9}$$

Which is referred to as the ‘element stiffness matrix’.

2.2 Torsional vibration

The energy expressions for the single torque element shown in Fig.1b are:

$$\begin{aligned} T_e &= \frac{1}{2}\int_{-a}^{+a} \rho \mathrm{I}_x \dot{\theta}_x^{\,2} dx \\ U_e &= \frac{1}{2}\int_{-a}^{+a} GJ\left(\frac{\partial \theta_x}{\partial x}\right)^2 dx \end{aligned} \tag{10}$$

The highest derivative appearing in these expressions is the first rotation about the x-axis, θ the variation of which is the same as the variation of u for an axial element. Which means the shape function of the torque element is also:

$$\mathrm{N}_i(\xi)=\frac{1}{2}(1+\xi_i\xi)\quad(\xi_1=-1,\xi_2=1) \tag{11}$$

The mass matrix and stiffness matrix of the single torque element can obtained by replacing ρA, EA by ρI_x, GJ respectively:

$$\begin{aligned}[m]_e&=\rho \mathrm{I}_x a\int_{-1}^{+1}\lfloor \mathrm{N}(\xi)\rfloor^{\mathrm{T}}\lfloor \mathrm{N}(\xi)\rfloor \mathrm{d}\xi\\ [\mathrm{K}]_e&=\frac{GJ}{a}\int_{-1}^{+1}\lfloor \mathrm{N}'(\xi)\rfloor^{\mathrm{T}}\lfloor \mathrm{N}'(\xi)\rfloor \mathrm{d}\xi\end{aligned} \tag{12}$$

2.3 Bending vibration

The deformation of a bending element is:

$$v=\lfloor \mathrm{N}(\xi)\rfloor\{v\}_e \tag{13}$$

where

$$\lfloor \mathrm{N}(\xi)\rfloor=\lfloor \mathrm{N}_1(\xi)\quad a\mathrm{N}_2(\xi)\quad \mathrm{N}_3(\xi)\quad a\mathrm{N}_4(\xi)\rfloor \tag{14}$$

The shape function of the bending element is:

$$\begin{aligned}\mathrm{N}_1(\xi)&=\frac{1}{4}(2-3\xi+\xi^3)\quad \mathrm{N}_2(\xi)=\frac{1}{4}(1-\xi-\xi^2+\xi^3)\\ \mathrm{N}_3(\xi)&=\frac{1}{4}(2+3\xi-\xi^3)\quad \mathrm{N}_4(\xi)=\frac{1}{4}(-1-\xi+\xi^2+\xi^3)\end{aligned} \tag{15}$$

The energy expressions for the single element shown in Fig.1c are

$$\begin{aligned}T_e&=\frac{1}{2}\int_{-a}^{+a}\rho A\dot{v}^2dx\\ U_e&=\frac{1}{2}\int_{-a}^{+a}EI_z\left(\frac{\partial^2 v}{\partial x^2}\right)^2dx\end{aligned} \tag{16}$$

Substituting the displacement expression into the energy expression gives the element mass matrix and the element stiffness matrix:

$$\begin{aligned}[m]_e&=\rho Aa\int_{-1}^{+1}\lfloor \mathrm{N}(\xi)\rfloor^{\mathrm{T}}\lfloor \mathrm{N}(\xi)\rfloor \mathrm{d}\xi\\ [\mathrm{K}]_e&=\frac{EI_z}{a^3}\int_{-1}^{+1}\lfloor \mathrm{N}''(\xi)\rfloor^{\mathrm{T}}\lfloor \mathrm{N}''(\xi)\rfloor \mathrm{d}\xi\end{aligned} \tag{17}$$

3. The formulation of proposed WFEM on 1D phononic crystals

The unit cell that forms the periodic structures is discretized by the Finite Element method. The mass and stiffness matrices M and K of the unit cell can be calculated by the shape function mentioned in section 2 or extracted from commercial FE package[5].

The nodal DOFs are defined as in Fig.2, which divided into: left right and internal DOFs. They are classified as $\begin{bmatrix}q_L & q_I & q_R\end{bmatrix}$.

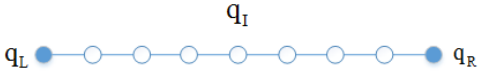

Figure 2 Mesoscopic scale of the unit cell

The nodal forces are classified in the same way.

3.1 Dynamical equation

As we all know, the dynamical equation expression for the unit cell shown in Fig.2 is:

$$\left(\mathrm{K}+i\omega\mathrm{C}-\omega^2\mathrm{M}\right)q=\mathrm{f} \tag{18}$$

In this paper, we ignore the damping of the structure, which means $\mathrm{C}=0$ .The dynamical equation of the unit cell can rewritten in the form:

$$\left(\begin{bmatrix}\mathrm{K}_{LL} & \mathrm{K}_{LI} & \mathrm{K}_{LR}\\ \mathrm{K}_{IL} & \mathrm{K}_{II} & \mathrm{K}_{IR}\\ \mathrm{K}_{RL} & \mathrm{K}_{RI} & \mathrm{K}_{RR}\end{bmatrix}-\omega^2\begin{bmatrix}\mathrm{M}_{LL} & \mathrm{M}_{LI} & \mathrm{M}_{LR}\\ \mathrm{M}_{IL} & \mathrm{M}_{II} & \mathrm{M}_{IR}\\ \mathrm{M}_{RL} & \mathrm{M}_{RI} & \mathrm{M}_{RR}\end{bmatrix}\right)\begin{pmatrix}q_L\\ q_I\\ q_R\end{pmatrix}=\begin{pmatrix}\mathrm{f}_L\\ \mathrm{f}_I\\ \mathrm{f}_R\end{pmatrix} \tag{19}$$

For free wave propagation, the internal force is zero, so $\mathrm{f}_I=0$.

3.2 Boundary conditions of the periodic structure

For 1D phononic crystals, the wave motion is characterized by the relationship between the boundary nodal DOFs and nodal forces of two adjacent unit cells. According to periodic structures theory, the DOFs are related as follows:

$$\mathrm{q}_R=\lambda_x\mathrm{q}_L \tag{20}$$

In addition, for free wave propagation, the sum of nodal forces of all elements connected to left nodal is zero, which leads to:

$$\mathrm{f}_L+\lambda_x^{-1}\mathrm{f}_R=0 \tag{21}$$

3.3 The WFEM formulation[6]

According to Eq. (20)， the DOFs of the unit cell $\begin{bmatrix}q_L & q_I & q_R\end{bmatrix}$ can be related to $\begin{bmatrix}q_L & q_I\end{bmatrix}$ using Φ_R, that is:

$$\begin{pmatrix}q_L\\ q_I\\ q_R\end{pmatrix}=\Phi_R\left(\lambda_x\right)\begin{pmatrix}q_L\\ q_I\end{pmatrix} \tag{22}$$

where

$$\Phi_R=\begin{bmatrix}\mathrm{I}_\mathrm{L} & 0\\ 0 & \mathrm{I}_\mathrm{I}\\ \lambda_x\mathrm{I}_\mathrm{L} & 0\end{bmatrix} \tag{23}$$

The sizes of q_L , q_I are L and I respectively. The matrices I_L and I_I in Φ_R represents the identity matrix of size L and I.

Similar to the force DOFs, according to Eq.(21):

$$\Phi_L\left(\lambda_x\right)\begin{pmatrix}\mathrm{f}_L\\ 0\\ \mathrm{f}_R\end{pmatrix}=0 \tag{24}$$

where

$$\Phi_L=\begin{bmatrix}\mathrm{I}_\mathrm{L} & 0 & \lambda_x^{-1}\mathrm{I}_\mathrm{L}\\ 0 & \mathrm{I}_\mathrm{I} & 0\end{bmatrix} \tag{25}$$

Then Eq. (19) can be rewritten as:

$$\Phi_L\left(\lambda_x\right)*\left(\mathrm{K}-\omega^2\mathrm{M}\right)*\Phi_R\left(\lambda_x\right)\begin{pmatrix}q_L\\ q_I\end{pmatrix}=0 \tag{26}$$

This expression includes two parameters ω and λ_x, here λ_x is fixed, and the value of ω are sought. Eq. (26) becomes a standard and linear eigenvalue problem of ω^2 as follows:

$$\left(\bar{\mathrm{K}}\left(\lambda_x\right)-\omega^2\bar{\mathrm{M}}\left(\lambda_x\right)\right)\begin{pmatrix}q_L\\q_I\end{pmatrix}=0 \tag{27}$$

where

$$\begin{aligned}\bar{\mathrm{K}}\left(\lambda_x\right)&=\Phi_L\left(\lambda_x\right)*\mathrm{K}*\Phi_R\left(\lambda_x\right)\\\bar{\mathrm{M}}\left(\lambda_x\right)&=\Phi_L\left(\lambda_x\right)*\mathrm{M}*\Phi_R\left(\lambda_x\right)\end{aligned} \tag{28}$$

3.4 Band gaps and wave shape

Vibration band gaps is one of the most representative dynamical performance of the phononic crystals. For a 1D phononic crystals, the irreducible zone of the 1st Brillouin zone is obvious. If the lattice constant of 1D phononic crystals is a, then the wave number $k_x \in \left(-\pi/a, \pi/a\right)$. The transmission coefficient $\lambda_x = \mathrm{e}^{-jka}$ is then obtained.

The mass and stiffness matrices M and K are symmetric positive definite matrices, in addition the matrix Φ_L is the conjugate transpose of the matrix Φ_R, thus the matrices $\bar{\mathrm{K}}\left(\lambda_x\right)$ and $\bar{\mathrm{M}}\left(\lambda_x\right)$ are positive definite Hermitian matrices.

Substituting the transmission coefficient λ_x into Eq. (27), the eigenvalue problem leads to the solutions $\left(\omega^2 \quad \phi'\right)$, with ω^2 real and positive, and vectors ϕ' orthogonal. The eigenvalue ω^2 give the frequency ranges of propagative wave. The eigenvectors ϕ' include only $\left[q_L \quad q_I\right]$, the wave shape ϕ for the phononic crystals are obtained by multiplying Φ_R:

$$\phi=\begin{pmatrix}\phi_L\\\phi_I\\\phi_R\end{pmatrix}=\Phi_R\phi' \tag{29}$$

4. Application example

In this section, the WFEM is applied to 1D phononic crystals. The vibration band gaps of the phononic crystals is obtained, the band gaps result is compared with the theory result, a good agreement is observed.

4.1 Axial vibration phononic crystal

An axial vibration phononic crystal is shown in Fig.3. The axial vibration beam is combined by two beams A and B. Beam A and beam B have the same diameter 0.005m, the same length 0.075m , their material are aluminum and epoxy respectively.

Lattice constant of this phononic crystal is 0.15m, the diameter of two beams is far less than the lattice constant, and only the axial vibration is considered here.

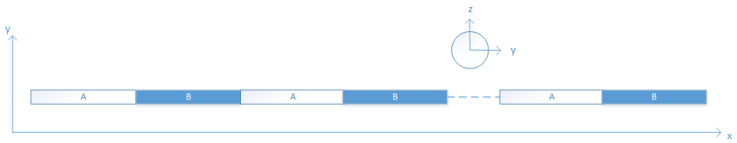

Figure 3 Axial vibration beam

Band structure of axial vibration phononic crystal is calculating by WFEM, and the result is shown in Fig.4.

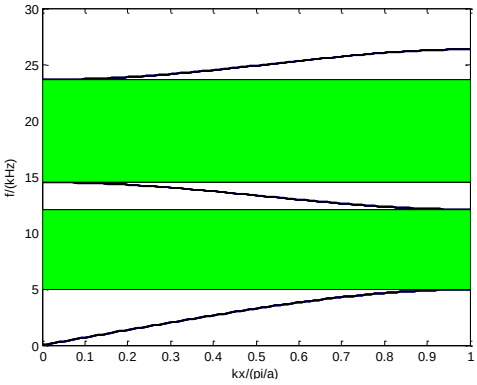

Figure 4 Band structure of axial vibration beam

The WFEM results are compared with the theory results, which is shown in Tab.1.

Table 1 Axial vibration band gap results

Axial vibration	Band gap 1 (kHz)	Band gap 1 (kHz)
WFEM	4.97-12.07	14.5-23.63
Theory	5.0-12.2	14.6-23.7
Error	-0.83%	-0.49%

It can be seen from Tab.1, a good agreement between WFEM results and theory results is observed.

4.2 Torsional vibration phononic crystal

A torsional vibration phononic crystal is shown in Fig.5. The torsional vibration beam is combined by two beams A and B. Beam A and beam B have the same ellipse cross section with the semi-major length 0.0707m and the semi-minor length 0.005m , the same length 0.075m , their material are aluminium and epoxy respectively.

Lattice constant of this phononic crystal is 0.15m, the diameter of two beams is far less than the lattice constant, and only the torsional vibration is considered here.

Figure 5 Torsional vibration beam

Band structure of torsional vibration phononic crystal is calculating by WFEM, and the result is shown in Fig.6.

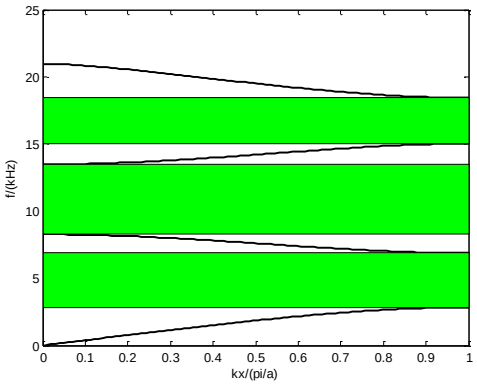

Figure 6 Band structure of torsional vibration beam

The WFEM results are compared with the theory results, which is shown in Tab.2.

Table 2 Torsional vibration band gap results

Torsional vibration	Band gap 1 (kHz)	Band gap 1 (kHz)	Band gap 3 (kHz)
WFEM	2.83-6.89	8.27-13.58	15.02-18.44
Theory	2.84-6.91	8.29-13.47	14.99-18.34
Error	-0.32%	0.29%	0.37%

It can be seen from Tab.2, a good agreement between WFEM results and theory results is observed.

4.3 Bending vibration phononic crystal

A bending vibration phononic crystal is shown in Fig.7. The bending vibration beam is combined by two beams A and B. Beam A has a rectangular cross-section with the width 0.01m and the height 0.01m, beam B has a rectangular cross-section with the width 0.01m and the height 0.005m, beam A has a length 0.05m, beam B has a length 0.02m, their material are aluminium and organic glass respectively.

Lattice constant of this phononic crystal is 0.07m, the size of two beams is far less than the lattice constant, and only the bending vibration is considered here.

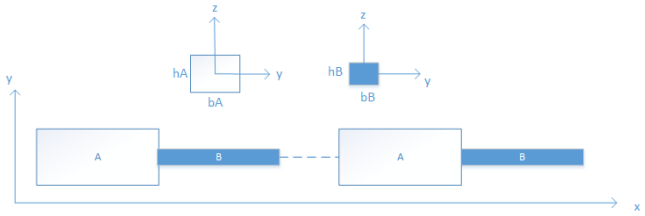

Figure 7 Bending vibration beam

Band structure of torsional vibration phononic crystal is calculating by WFEM, and the result is shown in Fig.8.

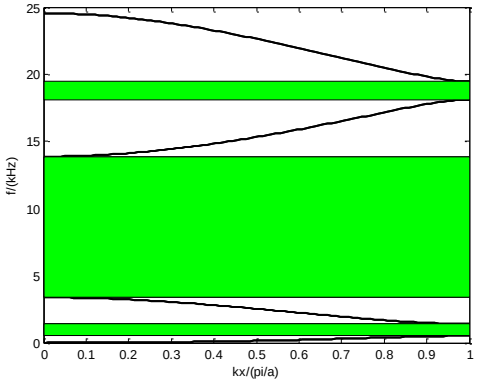

Figure 8 Band structure of bending vibration beam

The WFEM results are compared with the theory results, which is shown in Tab.3.

Table 3 Bending vibration band gap results

Bending vibration	Band gap 1 (kHz)	Band gap 1 (kHz)	Band gap 3 (kHz)
WFEM	523.6-1414.6	3.38-13.87	18.12-19.47
Theory	460-1390	3.2-12.58	/
Error	1.77%	5.6%	/

It can be seen from Tab.3, a good agreement between WFEM results and theory results is observed.

As a conclusion, three types of vibration mode of the phononic crystals are all proceeded by WFEM, and the results are compared with the theory results, a good agreement is observed. Which

means WFEM can be an effective instrument in calculating the vibrations band gaps of one-dimensional phononic crystals.

5. Conclusions

This paper employs the wave finite element method to acquire the vibration band gaps of one-dimensional phononic crystals. The mass and stiffness matrices of one-dimensional single element are proceeded by finite element displacement method. The formulation of WFEM on one-dimensional phononic crystals is provided. Three types of vibration mode of the one-dimensional phononic crystals are obtained by WFEM, the band gaps results are compared with the theory results, a good agreement is observed.

This work provides an effective technique to analyse the dynamical characteristics of metamaterial structures. Future investigations will address to the application of the WFEM on two-dimensional phononic crystals or more complex structures.

ACKNOWLEDGEMENTS

This work was supported by the National Key technologies Research &Development program under Grant No. 2016YFC0801702 and National key Basic Research Program of China (973 Program) under Grant No. 2013CB632905.

REFERENCES

1 Hussein, M. I., Leamy, M. J. and Ruzzene, M. Dynamics of Phononic Materials and Structures: Historical Origins, Recent Progress, and Future Outlook, *Applied Mechanics Reviews*, **66** (4), 040802-040802, (2014).

2 Li, C., Huang, D., Guo, J. and Nie, J. Engineering of band gap and cavity mode in phononic crystal strip waveguides, *Physics Letters A*, **377** (38), 2633-2637, (2013).

3 Li, Y., Shen, H., Zhang, L., Su, Y. and Yu, D. Control of low-frequency noise for piping systems via the design of coupled band gap of acoustic metamaterials, *Physics Letters A*, **380** (29-30), 2322-2328, (2016).

4 Mencik, J. M. and Ichchou, M. N. Multi-mode propagation and diffusion in structures through finite elements, *European Journal of Mechanics - A/Solids*, **24** (5), 877-898, (2005).

5 Mace, B. R., Duhamel, D., Brennan, M. J. and Hinke, L. Finite element prediction of wave motion in structural waveguides, *The Journal of the Acoustical Society of America*, **117** (5), 2835-2843, (2005).

6 Zhou, C. W., Lainé, J. P., Ichchou, M. N. and Zine, A. M. Multi-scale modelling for two-dimensional periodic structures using a combined mode/wave based approach, *Computers & Structures*, **154**, 145-162, (2015).